The AXAF HXDS germanium solid state detectors

W.C. McDermott[a], E.M. Kellogg[a], B.J. Wargelin[a], I.N. Evans[a], S.A. Vitek[a], E.Y Tsiang[a], D.A. Schwartz[a], R. Edgar[a], S. Kraft[b], F. Scholze[b], R. Thornagel[b], G. Ulm[b], M. Weisskopf[c], S. Odell[c], A. Tennant[c], J. Kolodziejczak[d], and G. Zirnstein[d]

[a] Smithsonian Astrophysical Observatory Cambridge, Massachusetts
[b] Physikalisch-Technische Bundesanstalt, Abbestr. 2-12 10587 Berlin,Germany
[c] Marshall Space Flight Center, Alabama
[d] USRA Huntsville, Alabama

ABSTRACT

The design, calibration, and performance of the High Purity Germanium (HPGe) solid state detectors (SSD's) used in the calibration of the Advanced X-ray Astrophysics Facility High Resolution Mirror Assembly (HRMA) is discussed. The focal plane SSD was used with various apertures to measure the point response function, as well as the effective area of the mirror. The good energy resolution of the detector allowed the effective energy of the mirrors to be measured with a single exposure using a continuum source. The energy resolution was also exploited in measuring the molecular contamination on the mirror surfaces.

The SSD's are the transfer detector standards for the HRMA calibration over the energy range from 700 eV to 10 keV. The calibration of the SSD's was performed mostly at the PTB radiometry laboratory using the electron storage ring BESSY. The spectral and spacial distribution of the undispersed synchrotron radiation can be calculated from first principles using the Schwinger Equation. With the electron storage ring being run in a reduced current mode of a few electrons, uncertainties in the calculated flux are below 1%. A comparison of the measured and calculated flux made it possible to determine the detector efficiency with an uncertainty of typically 1%. Electronic effects such as pile-up, count rate linearity and deadtime have been investigated.

Keywords: AXAF, solid state detectors, X-ray detectors, absolute calibration

1. INTRODUCTION

The HXDS solid state detectors (SSD) are a pair of germanium solid-state detector that serves as the primary transfer standard for the calibration of the High Resolution Mirror Assembly (HRMA) of the Advanced X-Ray Astrophysical Facility (AXAF) in the range from 700 eV to 10 keV. One detector was absolutely calibrated and served as a flux monitor during the ground based calibration of the HRMA. The other detector was used in the focal plane of the mirror and is being calibrated relative to the flux monitor. The good energy resolution of the detector allowed measurements such as molecular contaminaion, effective energy, and effective area of the detector to be made with a sigle exposure. Also, the large array of apertures incorporated into the detector allowed the srtucture of the focused beam from the mirror to be explored. These characteristics and calibration descriptions are presented in the sections that follow.

2. DETECTOR DESCRIPTION

The HXDS SSD, purchased from Canberra Industries, is a hybrid of their LEGe detector that has undergone modification by the Smithsonian Astrophysical Observatory (SAO). The detector consists of a high purity germanium crystal that is 6.2 mm in diameter and 5 mm thick. The active area of the detector is 30 cm^2. The front surface contact (P+) is made of 1000 angstroms of ion implanted aluminum. This contact extends around the sides of the crystal making the sides of the crystal conducting rather than insulating. The rear surface (N+) contact is a lithium diffused spot that does not cover the entire surface. This unique configuration reduces the capacitance of the detector and thus helps to reduce noise[1].

Visible light is blocked from reaching the Ge crystal via an infrared shield which consists of a 1000 angstroms of Al on 0.25 microns of paralyene. This brings the total amount of Al filtering to 2000 angtroms, (1000 A on the surface of the crystal and 1000 A on the IR Shield). The detector is also equipped with a 1 micron paralyene vacuum barrier. The primary purpose of this membrane was to provide the detector with it's own vacuum space in order to reduce the amount of contamination, including water vapor, that might reach the Ge crystal once the detector was mounted in the instrument chamber that housed the HRMA.

SPIE Vol. 3113 • 0277-786X/97/$10.00

The Ge crystal is mounted to a 1.2 liter all-attitude portable cryostat via a cold finger. The all-attitude cryostat allows positioning the detector in any direction without loss of cryogenic fluid. With proper evacuation of the cryostat, the cryogen would keep the detector cool without the need for a refill for 36 hours. Since the detector would ultimately be in a vacuum itself, the cryostat was specifically designed to be able to attach cryogenic fill lines that could be used to fill the detector even when cryostat was in vacuum. A schematic of the detector is shown in Fig. 1.

The front of the detector is fit with a computer controlled aperture wheel that contains 20 apertures. These aperture sizes range from 5 microns to 5 mm. They also include a 132 micron Al filter and a 27 micron Al filter which were used in the absolute calibration phase of the detector. The filter thicknesses were measured at the National Synchrotron Light Source (NSLS) using an in-out measurement over an energy range of 2 keV to 7 keV. Additionally, a ^{244}Cm source was placed in the aperture wheel to measure the ice build up on the Ge crystal that is inevitable with a cryogenically cooled detector. This source also served as a convenient way to check the gain of the detector system periodically during the HRMA calibration. This will be discussed further in a later section.

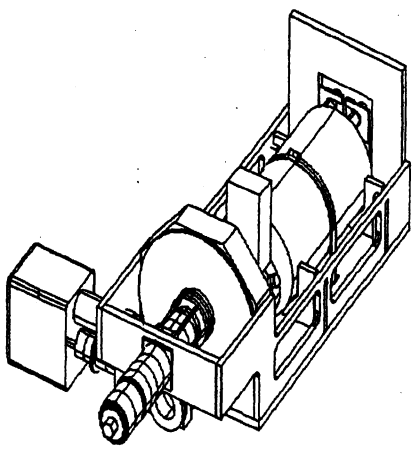

Figure. 1. Schematic of the HXDS Solid State detector

2.1 Signal Processing Electronics

The detector includes a pulsed optical resetting type preamplifier. This type of amplifier does not employ a feedback resistor which discharges the integrator portion of the preamp. This allows the charge to build up in the preamplifier. To reset the preamplifier to it's initial condition, an led is pulsed near the FET chip and discharges it. This reset rate was approximately one Hz. During this reset pulse, a veto signal is sent to the amplifier which disables it until the reset pulse has passed. Since this design eliminates the need for a feedback resistor, the noise in the preamp is much lower that a typical RC feedback type preamp making it idea for low energy detection[2]. The preamp provides two outputs which allow the detector to be connected to a shaping amplifier that is being run in a differential mode. This was necessary to limit noise pick up since the shaping amplifiers were located more than 50 feet from the detector.

An Ortec 671 shaping amplifier was used with an SAO built add-on that allowed the settings of the shaping amplifier to be set remotely via computer control. The unipolar output was connected to an Ortec 921 Multi-Channel Buffer that was also remotely computer controlled. The gain of the detector was set to give 5 eV/channel over 4096 channels. The shaping amplifier allowed shaping times selectable from 0.5 microseconds to 10 microseconds. However, during the calibration only two shaping time constants, 2 ms and 10ms, were utilized. The 2 ms shaping time was used when the counting rate was high (larger than 1500 Hz) while the 10 ms was used at lower counting rates.

The bias supply for the detector was a CAEN N470 quad high voltage power supply and was set at 485 volts. This unit was also controllable by computer commands. The bias supply included an input from the detector preamp that signalled a voltage shutdown when the detector started to warm up.

2.2 Deadtime Corrections

Deadtime corrections were planned to be made by using a pulser (Berkeley Nucleonics model BH-1) as an input signal that would suffer the same losses an x-ray event would suffer to first order. Since the pulser used was a repeating pulser, it was

unable to interfere with itself. This made it necessary to introduce second order statistical corrections to the data. This method was tested by using a radioactive source as a proof of principle and also at BESSY. The results of the pulser deadtime corrections were compared with the built in Gedke-Hale[3] deadtime correction circuitry that existed in the multichannel analyzer.

The pulser amplitude was set to channel that was high enough such that the recorded pulser peak could not be influenced by any recorded x-ray peaks. A digital counter was used to count the number of pulses that were injected into the preamp. A gate on the counter was connected to the MCA so that the counter would only count when the MCA was actively collecting. The radioactive source to detector distance was varied on each successive collection. The counts were summed, corrected for deadtime, and an activity of the source was calculated for each run. The results showed that the pulser method was capable of predicting the radioactive activity very accurately, whereas the Gedke-Hale system prediction varied by sometimes more than 8%.

A problem was discovered with the pulser method. When the pulser amplitude was set high, and the pulser rate was also relatively high (100Hz+), the pulser would cause a severe undershoot of the preamp. This would cause any x-ray event arriving after the pulser event to be recorded lower in energy that it should be. The resulting spectrum showed peak widths much broader than the detector was capable.

The problem could be remedied in one of the two ways. First, reduce the pulser amplitude to a level that would cause a minimal undershoot. This worked quite well, however the pulser was in a position that made spectroscopy at lower energies difficult. The second solution was to decrease the pulser frequency. This minimized the number of influences the pulser would have on the input x-ray rate.

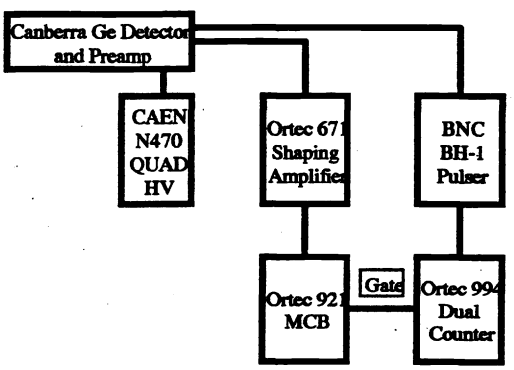

Figure 2. Schematic representation of the PHA chain with the deadtime correction counter

3. Absolute Calibration

The detector was calibrated using synchrotron radiation under a program developed by the Physikalishe-Techniche Bundesalant (PTB) at the electron storage ring BESSY[4]. The response function of the detector was measured at BESSY using dispersed synchrotron radiation from a monochromator system. In the energy range from 1.1 keV to 5.9 keV a double crystal monochromator was used. The upper energy was limited by mirror optics in the beamline. The lower energy was limited by the Bragg angle of the crystals used in the monochromator. In order to get as pure a single line as possible, the second crystal of the monochromator was slightly detuned from the first crystal. This suppress much of the harmonic contamination.

For energies from 600 eV to 1.1 keV, the spectral response function was measured at a grating monochromator beamline. Stray light and second order contamination effects from the monochromator were suppressed by the use of filtering. This beamline consists of an SX-700 grating monochromator with calibrated photodiodes for measuring the beam intensity downstream from the monochromator. This made it possible to simultaneously measure the detector efficiency as a function of energy. Since the monochromator was capable of reach 1.7 keV, response function data and detector efficiency data were collect up to this energy point.

The response function of the detector consists mainly of a peak and a lower energy shelf. The peak is obviously derived from a photon depositing all of it energy in the Ge crystal and being collect without loss. The shelf arises from the photon creating

photoelectrons at the surface of the crystal. These electrons must traverse the dead layer until they are collect as a charge. Since the mean free path for the electrons is very short in the crystal, not all of the electrons are collected. This incomplete-charge collection results in a recorded event in an energy bin lower than the characteristic photon energy.

The absolute detector efficiency was measured at BESSY using *undispersed* synchrotron radiation. The absolute flux from the storage ring was calculated from first principles using the Schwinger equation. Precise measurement of the magnetic field, ring current, source distance and aperture size allow this calculation to be made.

The storage ring is injected with a few milliamps of current and the orbit is allowed to stabilize for a couple of hours. Once the orbit is stabilize, the source size is measured. This is done by scanning a polarizing crystal through the x-ray beam. Once the source size is measured, the energy of the electron beam is determined by injecting an RF signal perpendicular to the electron orbit. The RF frequency is adjusted until it is resonant with the electrons in the storage ring.

After these parameters are found, the ring current is reduced by partially placing a baffle in the storage ring. This blocking plate removes some of the electrons from the orbit. Once the ring current is reduced to a few electrons, data may be taken. As the current is stepped down, it is possible to observe individual electrons being removed once the current gets down to the 10^3 electron mark.

4. DISCUSSION OF CALIBRATION RESULTS

4.1 Response Function

A number of interesting features became apparent during the measurement of the response function at the double crystal monochromator beamline. As the energy of the monochromator was scanned through the Ge L III edge, the number of counts that appeared in the shelf increased. This is shown in fig. (FIG) Since the crystal is more "absorbing" around the Ge-LIII edge, more the photons suffer from an incomplete charge collection as was described above. This effect was not observable in the other Ge-L edges. However, similar effects were observed when the monochromator was scanned across the Al-K edge, due to the front surface contact in the Ge crystal, and across the Ge-K edge. (see Fig . 3.)

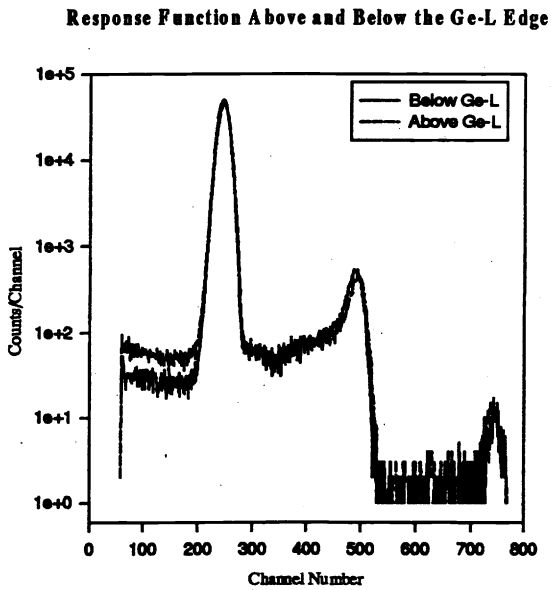

Figure 3. Pulse-height spectrum showing the change in the shelf as the monochromator is scanned across the Ge-L III edge.

Some other features that are observable in the response function are the presence of an Al fluorescence peak in the shelf of the spectrum when the input photon energy was larger than 1.5 keV. Again, this arises from the Al infrared shield and the Al coating on the front of the crystal. Also when the photon energy is larger than the Ge-L edge, a Ge-L escape peak is present in the shelf. Both of these features are shown in fig. %%%. These two features can help set the gain of the detector

independent of the ^{244}Cm source that was housed in the aperture wheel of the detector.

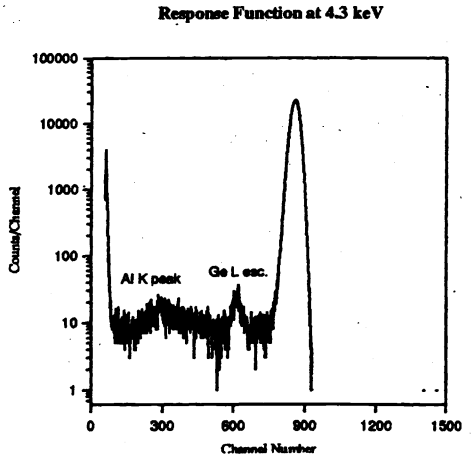

Figure 4. Pulse-height spectrum showing the Al flourescence peak and the Ge-L escape peak.

In spectra collected using a monochromator with an input photon energy less than the Al absorption edge, the Al fluorescence peak has been instrumental in determining the origin of counts that are recorded at higher in energies. Originally the counts were thought to be due primarily to pile-up. However with the presence of the Al fluorescence peak, it is clear that some of the counts are actual higher energy photons (perhaps second order).

The response function of the detector was relatively good. Typically the resolution was less than 170 eV at 5.9 keV using a 10 μsec shaping time constant. The reason the detector did not perform better than this is because of a moderate leakage current that introduced noise in the preamp and broadened the resolution of the detector. Also, the local noise environment at the synchrotron was relatively large.

4.2 Detector Efficiency

The detector efficiency was measured using both a calibrated photodiode as a transfer standard, and by exposing the detector to undispersed synchrotron radiation in which the flux was calculated from first principles. The calibrated photodiode was used with an SX-700 grating monochromator beamline so that the detector efficiency could be measured as function of input energy. Detailed measurements of the fine structure of the Al infrared shield and front surface coating could be made using this beamline. The raw data summed over the x-ray peak and shelf are shown on fig ***. The data were also corrected to first order for deadtime using the pulser method.

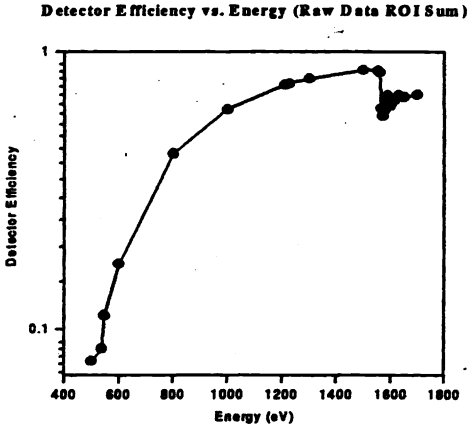

Figure 5. Detector Efficiency vs. Energy from SX-700 data.

The calibration data taken at the SX-700 beamline proved useful in determining the uniformity over the surface of the crystal.

Data was taken with the monochromator set on the three energies (Above Al-K, below Al-K and at 600 eV). The data were normalized to the photon flux measured by a calibrated photodiode. The monochromatic beam was collimated by an aperture to a 1 mm spot that was scanned over the surface of the crystal in a two dimensional raster scan. The results showed a 3% variation in the efficiency of the crystal. All three scans showed the same results. Since two of the scans were done above and below the Alike edge, this non-uniformity in the efficiency does not seem to be do to the IR filter and Al coating on the crystal.

The absolute flux from the undispersed synchrotron radiation was calculated from first principles using the Schwinger Equation. This requires a knowledge of the certain experimental parameters such at the beam current, electron energy, path length to the detector, inclination of the detector with respect to the electron orbit, and the strength of the magnetic field in the bending magnet. The uncertainty of measuring these parameters at BESSY add in quadrature to be less than 1%.

The electron ring at BESSY was operated with a electron energy of 850 MeV. This gives a critical energy of &&&&. This means that most of the photons were primarily in the lower energy bins. As a results, the detector spends most of its time counting these low energy photons. In order to get reasonable statistics at the higher energies, the Al filters in the aperture wheel were use to suppress the counting of the lower energy signal. The use of these filters effectively "shifted" the energy of the input synchrotron radiation and allowed a calibration of the detector at higher energies (10 keV).

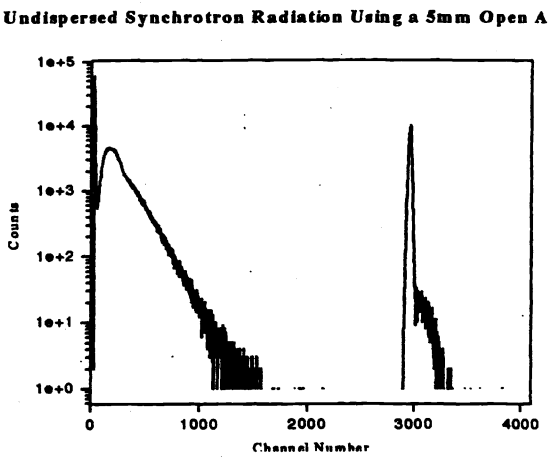

Figure 6. Undispersed synchrotron radiation using a 5 mm open aperture.

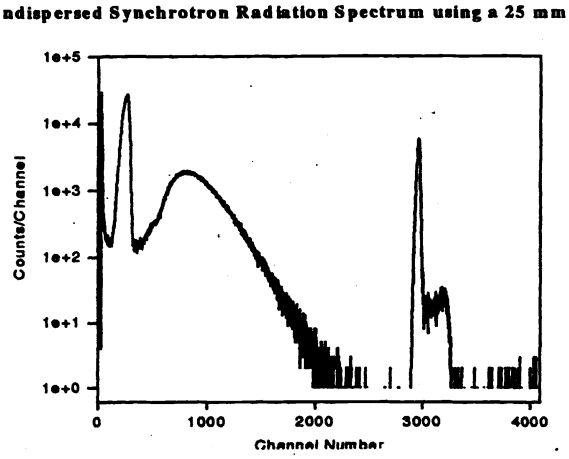

Figure 7. Undispersed synchrotron radiation using a 25 mm Al filter. The filter "shifts" the photon spectrum to a higher energy.

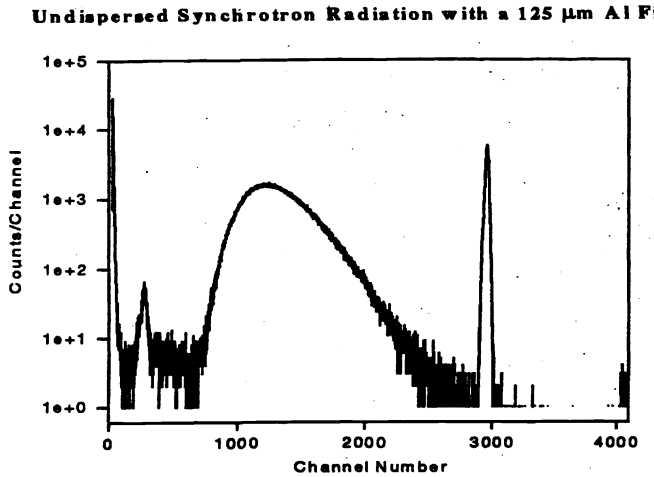

Figure 8. Undispersed synchotron radiation spectrum using a 125 mm Al filter. This filter allows a calibration up to 10 keV.

The detector efficiency was measured in such a way that any filters used during data collection were considered to be part of the detector instead of calibrating each individual component. However, the ice build up on the crystal was a variable than needed to be measured. A radioactive ^{244}Cm source with and Fe target was placed in the aperture wheel to help measure this ice thickness. When the alpha particles form the ^{244}Cm source impinged on the Fe target, it fluoresced both the Fe-K and Fe-L lines. The ratio of the Fe-L strength to Fe-K strength measured over time was used to calculate the ice thickness (see fig. ***). Another advantage of the ^{244}Cm source was the ability to measure the gain of the detector at any time. The source is rich in lines resulting not only from the Fe fluorescence, but also from the emission of Pu L lines that are a result of the daughter products of the ^{244}Cm decay.

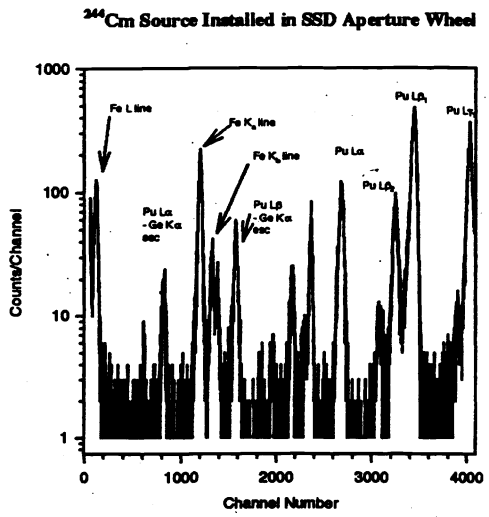

Figure 9. ^{244}Cm spectrum used to determine the ice layer thickness. This is allow useful for monitoring the gain.

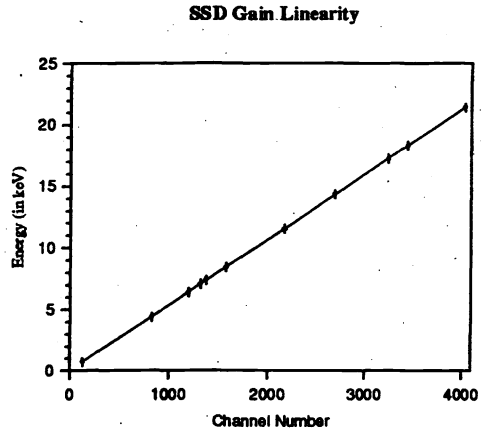

Figure 10. Gain vs. Energy. This data was obtained from the ^{244}Cm source.

5. USES OF THE SSD DURING THE HRMA GROUND CALIBRATION

As stated earlier, the good energy resolution of the SSD's allowed one exposure measurements during calibration of the HRMA. One such measurement is a molecular contamination measure. During this measurement, an electron impact source with a C target was run with a potential of 15 kV. This produced a relatively clean continuum spectrum that illuminated the mirror surface and flouresced any contamination that might have been on th surface. One such spectrum from the molecular contamination studies is shown in Fig. 11. Simlar sources setting were used to measure the effective area of the HRMA.

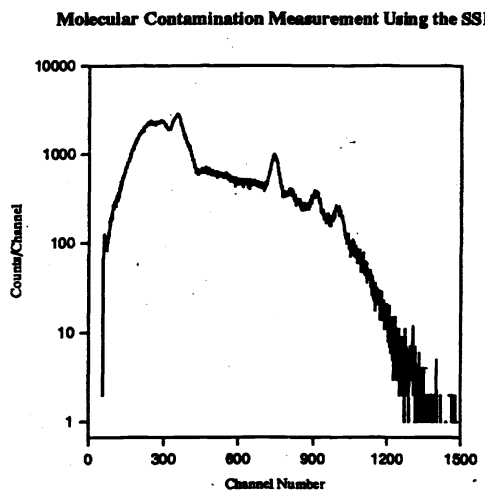

Figure 11. SSD Spectrum from Molecular Contamination studies during HRMA calibration.

ACKNOWLEDGEMENTS

We wish to thank all of the HXDS Mission Support Team. Special thanks go to Tim Norton, Roger Eng, Mark Ordway, John Moran, Nicholas Mistry, and Stephen Keleti for their design, and implemintation of the hardware and software systems of the HXDS. We also wish to thank the High Energy Astrophysics Division of the Smithsonian Astrophysical Observatory. This work was performed under the auspices of the National Aeronautics and Space Administration by the AXAF Mission Support Team under Contract No. NAS8 40224.

REFERENCES

[1] Canberra Industries, "Germanium Detectors", Sec. 1.5, 1992
[2] G. F. Knoll, "Radiation Detection and Measurement",(New york: John Wiley and Sons), p. 592-4, 1989
[3] R. Jenkins, R.W. Gould, and D. Gedcke, Quantitative X-Ray Spectrometry (New York: Marcel Dekker, Inc.), 1981, pp266-267
[4] F. Sholze, G. Ulm, Nucl. Instr. and Meth. A 339 p.49